

# Letters

## Analysis and Processing of Ultra Wide-Band SAR Imagery for Buried Landmine Detection

David Wong and Lawrence Carin

**Abstract**—Experimental and theoretical results are presented for ultra wide-band (UWB) synthetic aperture radar (SAR) signatures of buried anti-tank and anti-personnel mines. Such are characterized by resonance-like peaks as well as valleys, across the 50–1200 MHz bandwidth considered. Consequently, frequency subbanding is used to highlight one target over another, of application to discriminating targets (mines) from clutter.

**Index Terms**—Buried object detection, synthetic aperture radar.

Ultra wide-band (UWB) synthetic aperture radar (SAR) is a new tool that has shown effectiveness for the detection of targets buried underground [1]. To examine the expected UWB SAR frequency-dependent signatures of buried landmines, we have developed a method-of-moments (MoM) algorithm, which models the target as a conducting body of revolution (BOR) embedded in a lossy dielectric half-space. The details of the MoM algorithm have been discussed elsewhere [3], [4]. The focus of this work is to demonstrate that: 1) close agreement is achievable between theoretical and experimental landmine signatures despite the complexity of the mines and the surrounding environment and 2) results from the models can be used to dictate which frequency bands are optimal for the detection of particular target classes.

The theoretical and experimental data correspond to landmines buried at Yuma Proving Grounds, Yuma, AZ. Soil samples were taken from this site from which the complex dielectric constant was measured. The results of the frequency-dependent soil characterization is shown in Fig. 1, with the measurements performed via a conventional coaxial probe [4]. These data correspond to a moisture content of 5% by weight, which is felt representative of the characteristics of this generally dry soil.

The two landmines considered here (both primarily metal) are an M20 anti-tank mine, which we consider buried to a depth of 15.24 cm, and a Valmara anti-personnel mine, buried just under the surface. Both targets approximate BOR's. In the computations, the target axis must be perpendicular to the air-ground interface such that the target half-space composite preserves the BOR symmetry [3], [4]. While this is clearly a simplification, in practice, landmines are generally so buried. Space limitations preclude a detailed accounting of the dimensions of these mines, but we note that the M20 anti-tank mine has an outer diameter of 33 cm and a total height of 17.5 cm, while the Valmara anti-personnel mine has an outer diameter of 10.16 cm and a total height of 20.32 cm (pictures of the mines are inserted in Fig. 2). With regard to the Valmara, note that it has several protruding metal spikes, which are not included in the BOR model. These prongs

Manuscript received January 18, 1998.

D. Wong is with the Army Research Laboratory, AMSRL-SE-RU, Adelphi, MD 20783 USA.

L. Carin is with the Department of Electrical and Computer Engineering, Duke University, Durham, NC 27708 USA.

Publisher Item Identifier S 0018-926X(98)08899-1.

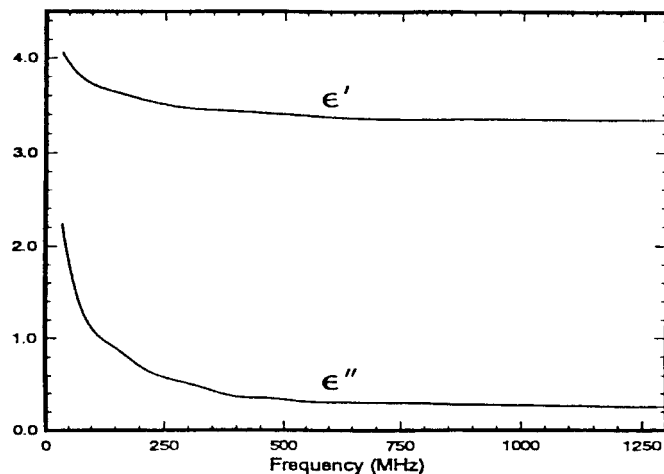


Fig. 1. Real ( $\epsilon'$ ) and imaginary ( $\epsilon''$ ) part of the complex dielectric constant for Yuma soil.

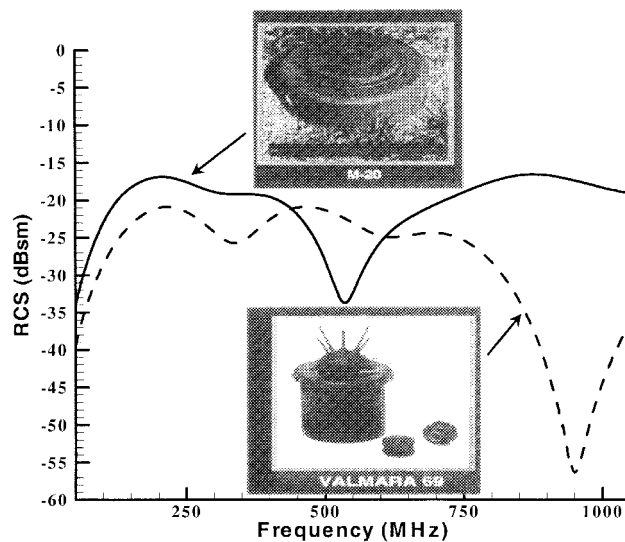


Fig. 2. Theoretical radar cross section (RCS) of the M20 and Valmara mines as a function of frequency for an incidence angle of  $30^\circ$  with respect to grazing.

are each approximately 10 cm in length and are likely to become most important at higher frequencies, when one approaches their resonant regime ( $\sim 1$  GHz for the soils considered). Although not considered here, the BOR model can be modified in principle to more accurately model the Valmara's prongs [5]. With regard to the UWB SAR system, details can be found in [1] and [2]. We note that the system operates over the 50–1200 MHz bandwidth, with measurements performed directly in the time domain.

In Fig. 2, we consider the theoretical RCS for the M20 and Valmara mines (VV (vertical-vertical) polarization), with results presented here for  $\theta_i = 30^\circ$ . Note that the RCS of the M20 mine

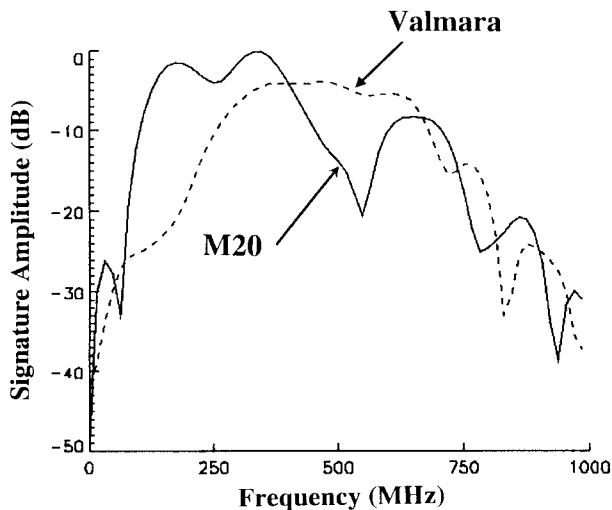


Fig. 3. Spectrum of the scattered signals from M20 and Valmara mines, as extracted from measured SAR imagery.

is characterized by two subbands over which the scattered fields are relatively large (approximately 160–400 MHz and 680–920 MHz), as well as an intervening subband over which the RCS is quite small (approximately 440–600 MHz). The two frequency subbands over which the RCS is large are representative of target resonances. Considering the first resonant band, a complex resonant frequency [4] with real part near 300 MHz (the center of this band) corresponds to a half wavelength of approximately 30 cm for the soil in Fig. 1, consistent with the general size (diameter) of the M20 mine. The broad frequency extent of this resonance-like feature is also consistent with that expected for a very low  $Q$  target [4].

The Valmara anti-personnel mine is considerably smaller than the M20 anti-tank mine and, therefore, one would expect its RCS to be smaller as well. However, from Fig. 2 we see that the RCS of the Valmara is, in fact, larger than that of the M20 in the frequency subband for which the M20 has a null (480–600 MHz). To examine whether these theoretical observations are manifested in actual SAR imagery, we consider the *experimental* spectrum of these two mines. Several rows of M20 and Valmara mines were buried in the Yuma soil, with burial depths as discussed above. From the measured (bipolar) SAR imagery [1], [2], one-dimensional down-range cuts (of 5-m length) were taken through ground-truth-dictated target positions. By taking into account the speed of light, these down-range cuts can be viewed as time-domain waveforms and are Fourier transformed to produce the spectrums in Fig. 3. Although we considered numerous examples of each mine, the general features of the results in Fig. 3 were faithfully reproduced. We see from Fig. 3 that the experimental spectrum of the M20 mine is characterized as in Fig. 2 by two resonant-like broad peaks separated by a sharp null. Moreover, over much of the spectrum the response of the M20 mine is larger than that of the Valmara, except in the region of the null in the M20 response.

The agreement between Figs. 2 and 3 is good, especially considering the following issues. While the RCS calculations in Fig. 2 have calibrated out the effects of the incident waveform, in practice, it is difficult to know the antenna response exactly. Therefore, the results in Fig. 3 are contaminated by the response of the antenna and, therefore, do *not* explicitly represent RCS (although the antenna spectrum is believed to be relatively flat over the bandwidth and imaging angle considered [1]). Moreover, since the results in Fig. 3 were extracted from a SAR image, they are not characterized by a single angle of incidence (angles from  $\theta_i = 20^\circ$  to  $\theta_i = 40^\circ$  are superposed when forming a single SAR image). The imaging

process itself introduces artifacts [1]. Additionally, while every effort was made to make the experimental parameters the same as those considered in the model, the local soil properties are unlikely to be exactly like those in Fig. 1 and there was likely variability in the exact mine placement (depth and orientation). Finally, recall that the BOR model did not account for the metal prongs atop the Valmara, which may explain why the very sharp dip in the theoretical Valmara RCS for frequencies near 1 GHz is not as obvious in the measured data (i.e., wire resonances with such not accounted for in the theory, may explain this discrepancy). Nevertheless, at frequencies less than approximately 850 MHz, the general agreement between theory and experiment is encouraging.

Based on the above theoretical and experimental evidence, instead of utilizing the full 50–1200 MHz bandwidth to form an SAR image, we perform frequency-domain filtering of the measured data from which subbanded SAR images are formed. A tapered finite-impulse response (FIR) filter was used to process the following subbands: 100–200 MHz, 200–500 MHz, 480–580 MHz, 700–1000 MHz. From Figs. 2 and 3, the RCS of the M20 is larger than that of the Valmara for all but the 480–580 MHz subband. Space limitations prohibit presentation of each of the subband images, but we summarize the results as follows. We calculated the energy associated with each mine, as extracted from the particular subband SAR images. On average, for the 100–200 MHz, 200–500 MHz, and 700–1000 MHz subbands, the energy in the M20 mine was, respectively, 10.2, 2.6 and 3.2 dB larger than that of the Valmara mines. For the 480–580 MHz subband, approximately representative of the null in the M20 response (Figs. 2 and 3), the Valmara mine had an energy on average 1-dB larger than that of the M20 mine. The relative energies summarized above are as expected from the data in Figs. 2 and 3, except for the 480–580 MHz subband for which the discrepancy in the Valmara and M20 energies may have been expected to be larger. We attribute this to the fact that the width of the measured null (Fig. 3) is smaller than that of the theory (Fig. 2) with which the subband filters were designed. Nevertheless, the general expectations have been confirmed, despite the complexity of the theory and measurements.

#### REFERENCES

- [1] M. A. Ressler and J. W. McCorkle, "Evolution of the army research laboratory ultra-wideband test bed," in *Ultra-Wideband Short-Pulse Electromagnetics 2*, L. Carin and L. B. Felsen, Eds. New York: Plenum, 1995, pp. 109–123.
- [2] S. Vitebskiy, L. Carin, M. Ressler, and F. Le, "Ultra-wideband, short-pulse ground-penetrating radar: Theory and measurement," *IEEE Trans. Geosci. Remote Sensing*, vol. 35, pp. 762–772, May 1997.
- [3] S. Vitebskiy and L. Carin, "Short-pulse plane wave scattering from a buried perfectly conducting body of revolution," *IEEE Trans. Antennas Propagat.*, vol. 44, pp. 112–120, Feb. 1996.
- [4] S. Vitebskiy, K. Sturgess, and L. Carin, "Late-time resonant frequencies of buried bodies of revolution," *IEEE Trans. Antennas Propagat.*, vol. 44, pp. 1575–1583, Dec. 1996.
- [5] T. E. Durham and C. G. Christodoulou, "A method for treating junctions between bodies of revolution and arbitrary surfaces," *IEEE Trans. Antennas Propagat.*, vol. 42, pp. 213–219, Feb. 1994.